

Influence of inter-and inter-pair distance of electrode arrays on tumor treatment

Abstract

Electrochemical therapy (EChT) is used for the treatment of cancer. The application of this therapy is simple, safe, effective and induces minimal adverse events in the organism. The objective is to evaluate the induced effectiveness of the distance of the electrode arrays (single and multiple pairs) for the quantification of the percentage of tumor destruction (PDT). A computer program was used for the calculation and simulation of PDT and a sample of (24 male and 24 female) BALB/c/Cenp laboratory mice. It is concluded that this therapy is effective for the treatment of tumors since the percentage of tissue damage increases; by more than 80% at a distance ($0.5 \leq d \leq 1$) cm from the electrode arrays inserted perpendicularly in the tumor geometry, which allows its use for the treatment of different types of tumors.

Keywords: tumor treatment, electric field, electrode arrays, electric field, tissue damage

Volume 8 Issue 4- 2024

Leonardo Mesa Torres,¹ Ivelice Gonzales Delgado,² Enaide Maine Calzado,³ Jorge Luis García Rodríguez,⁴ Luis Enrique Bergues Cabrales⁵

¹Master en Ciencias, Ingeniero Mecánico, Profesor Instructor, Centro Nacional de Electromagnetismo Aplicado, Universidad de Oriente, Cuba

²Departamento de Telecomunicaciones, Facultad de Ingeniería Eléctrica, Universidad de Oriente, Cuba

³Master en Ciencias, Ingeniero en Telecomunicaciones, Profesor Auxiliar, Departamento de Telecomunicaciones, Facultad de Ingeniería Eléctrica, Universidad de Oriente, Cuba

⁴Master en Ciencias, Licenciado en Mecánica, Profesor Auxiliar, Centro Nacional de Electromagnetismo Aplicado, Universidad de Oriente, Cuba

⁵Doctor en Ciencias Biológicas, Licenciado en Física, Profesor Titular, Centro Nacional de Electromagnetismo Aplicado, Universidad de Oriente, Cuba

Correspondence: Leonardo Mesa Torres Master en Ciencias, Ingeniero Mecánico, Profesor Instructor, Centro Nacional de Electromagnetismo Aplicado, Universidad de Oriente, Santiago de Cuba 90400, Cuba, Email leonardito@uo.edu.cu, leonardomesatorres084@gmail.com

Received: December 16, 2024 | **Published:** December 24, 2024

Introduction

Electrolytic ablation therapy or electrochemical therapy (EChT) consists of the application of direct electric current of very low intensity to the tumor by means of the insertion of two or more electrodes in its interior and/or vicinity.¹ The first experiences in Cuba on the use of EA on tumors were reported in.^{2,3} In recent years, the use of different types of physical anti-cancer therapies has become increasingly popular, such as electroporation,¹ hyperthermia,² laser,³ electrochemical therapy (EChT)^{4,5} and E2 therapy (EChT+electroporation).⁶ EChT is simple, safe, effective, and induces minimal adverse events in the organism and constitutes another option when established anti-cancer therapies (surgery, radiotherapy, chemotherapy and immunotherapy) fail or cannot be applied due to the patient's general condition; therefore, it can be used prior to surgery to reduce the size of the tumor and combined with radiotherapy and chemotherapy, which reduces the doses usually used by these conventional therapies by 10%.⁷ However, two studies.^{8,9} report the death of several BALB/c/Cenp mice carrying highly aggressive and metastatic F3II mammary carcinoma. The death of these animals is essentially due to metastasis in the lung and other organs (liver and kidney) and to a lesser extent to EChT; since their overall effectiveness (partial remission + complete remission) is greater than 60%, in agreement with preclinical,^{10,11} and clinical results.⁷ This type of antitumor treatment has not been as well recognized and standardized as the established oncospecific therapies mentioned above and its mechanism of action is poorly understood, despite these deaths. The non-standardization of this type of therapy is due to the fact that the optimal dose and configuration of electrodes

(single and multiple pairs) inserted into the tumor geometry have not been established.⁵⁻⁹ Long experimentation times and considerable material resources are required to understand these aspects if they are undertaken only from the experimental point of view. Therefore, physical-mathematical modeling is suggested as a fast and feasible way.^{8,9} The Cuban Bioelectricity group focuses its efforts in proposing different two-dimensional (2D),¹²⁻¹⁵ and three-dimensional (3D),^{16,17} physical-mathematical models that allow knowing the spatial distributions of the electric potential (Φ), the intensity of the electric field (E), electric current density (J), temperature (T), pH fronts, and the percentage of PDT tissue damage generated by different geometries of single electrodes,^{12,13,15-17} or multiple pairs of electrodes inserted collinearly or not in the tumor.¹⁴ Experimental results in *in vitro*, preclinical and clinical studies, and simulations obtained in current mode of EChT are similar to those in electrical voltage mode. The electric current mode consists in that the intensity of the direct electric current remains constant during its application; however, the electric voltage changes due to the variation of the electrical resistance of the tumor. The electrical voltage mode consists in that the electrical voltage remains constant during its application; however, the intensity of the electrical current changes due to the variation of the electrical resistance of the tumor; in both modes of EChT can be explained by the toxic products produced by electrochemical reactions, tissue damage (by apoptosis and necrosis) and other biophysical-chemical processes that are induced in the tumor.^{17,19-23} It is important to note that the bioeffects and efficacies/effectivities are similar when both modes of EChT are used in mice¹⁰ and humans.¹⁷ Amount of electric charge (Q) 80 C/cm³ and potential difference (ΔV_0) between 10

and 12 V are the doses that induce the highest antitumor efficacies on different tumor types when EChT is used in current and voltage-gated mode, respectively.¹⁴ These electrode configurations have been experimentally validated in tumors,^{7-10, 18,19} potato,^{13,20} in silico,¹³ and in vitro.²¹ Calzado et al.¹⁴ as they report the spatial distributions of electric potential (Φ), electric field strength (E), electric current density (J), temperature (T), pH fronts, on tumor geometry; Currently, in the scientific literature there are no reports of the influence of the distance (d) of single and multiple pair electrode array configurations on the (PDT).

Material and methods

In this study, the following were used forty-eight BALB/c/Cenp male and female mice (24 males and 24 females), 6–7 week old and 18–20g mass, supplied by the (CENPALAB, Havana, Cuba), were used, (Registration number 16/17, code AETM0917, 17 May 2017), guidelines animal ethic comission of República de Cuba and Council Directive 86/609/ECC of 24 November 1986, which followed guidelines for the welfare of animals in experimental neoplasia con platinum needle electrodes are inserted parallel to the z axis. ONCOCED B&E-01 electrostimulator designed and built by researchers at Centro de Biofísica Médica, Centro Provincial de Electromedicina and Centro Nacional de Electromagnetismo Aplicado (CNEA), all from Santiago de Cuba, Cuba. was used for DC treatment. This equipment was calibrated with a calibrator (Bodystat15-MDD device, Tampa, FL) before, during, and after DC treatment to evaluate its stability. This calibrator (courtesy of Ing. Antonio Gómez Yépez, Grupo de Terapia Metabólica, Veracruz, México) had an electric resistance of $500 \pm 0.1V$ [Lafargue et al., 2013]. The electrical voltage (in V), DC intensity (in mA), and electrical charge (in C) were monitored every 2min during treatment. Stainless steel electrodes of $0.5 \leq d \leq 1mm$ diameter and 68.5mm long were used. Electrode material was AISI 316L austenitic stainless steel (Jiangsu Shenghengte Stainless Steel, Wuxi, China).

In the Figure 1 shows the single and multiple pair electrode arrays used in the experiment.

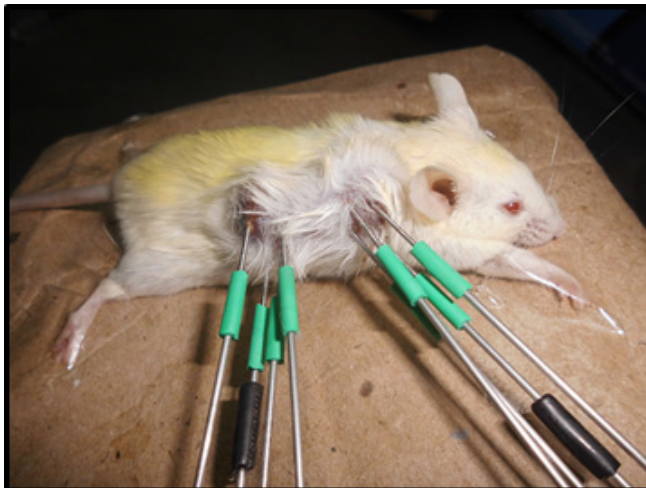


Figure 1 Tratamiento Dc tumor cells in the BALB/c/Cenp mice.^{9,14}

Figure 2 shows the studies performed for the configuration of collinear electrodes inserted perpendicularly to the tumor at a distance $d = 0.5; 0.7$ and 1.0 cm called: b) C_i -Ia, C_i -Ib, c) C_i -Ic and d) C_p -II and multiple pairs of electrodes inserted concentrically at $45; 135; 225$ and 315° respectively, with respect to the x-axis.^{13,14}

A group of multiple anodes and cathodes inserted individually and perpendicularly along the tumor diameter of radius $R = 2.5$ cm separated at a distance (d) of $0.5, 0.7$ and 1 cm, named C_i -Ia, C_i -Ib

and C_i -Ic, respectively; and the concentric one, with the electrodes located at $45, 135, 225$ and 315° , referenced as C_i -II, were simulated. The configurations of multiple straight needle electrodes were shown in Table 1 (Configurations C_i -Ia, C_i -Ib, C_i -Ic and C_i -II). The insertion depth of the electrodes was along the $z = 0$ axis.

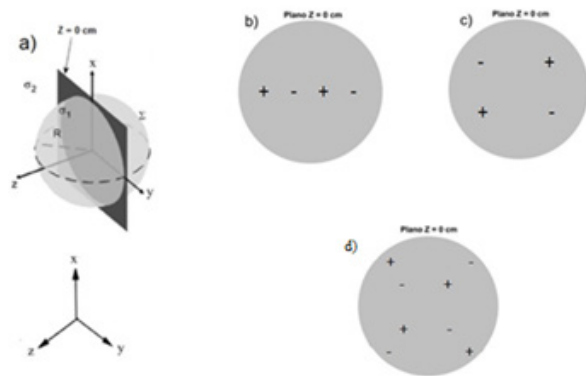


Figure 2 Different electrode configurations inserted in the tumor: a) Schematic representation of a spherical tumor. Electrode configurations: b) C_i -Ia, C_i -Ib, c) C_i -Ic, d) C_p -II.

Table 1 Parameters for configurations C_i -Ia, C_i -Ib, C_i -Ic, C_p -I and C_p -II

Electrode arrangement	Parameters		
	Quantity	Polarity	Positioning
C_i -Ia	4	Electrodes 1 and 3 (positive) and electrodes 2 and 4 (negative) a	Collinear electrodes, $d = 0.5$ cm.
C_i -Ib	4	Electrodes 1 and 3 (positive) and electrodes 2 and 4 (negative) a	Collinear electrodes, $d = 0.7$ cm.
C_i -Ic	4	Electrodes 1 and 3 (positive) and electrodes 2 and 4 (negative) a	Collinear electrodes, $d = 1$ cm.
C_i -II	4	Electrodes 1 and 3 (positive) and electrodes 2 and 4 (negative) b	Concentric electrodes 1; 2; 3 and 4 placed at $45; 135; 225$ and 315° , respectively, with respect to the x-axis.
C_p -I		Electrodes 1 and 3 (positive) and electrodes 2 and 4 (negative) b	Pairs of colonial electrodes, $d = 1$ cm
C_p -II	8	Electrodes 1; 3; 5 and 7 (positive) and electrodes 2; 4; 6 and 8 (negative) b	Concentric electrode pairs 1-2; 3-4; 5-6 and 7-8 placed at $45; 135; 225$ and 315° with respect to the x-axis, respectively.

The calculation and simulation of the percentage of tissue damage (TDP_i , in %) that is induced in the tumor ($i = 1$) and in the surrounding healthy tissue ($i = 2$) was performed by the following equation.

$$TDP_i = \frac{N D_i}{N T} 100 \% \tag{1}$$

where ND_i is the number of points satisfying the condition $T \geq 42$ °C and NT_i the total number of points in the tumor ($i = 1$) and in the surrounding healthy tissue ($i = 2$). N_T is calculated in the entire tumor volume of $R = 2.5$ cm ($N_{T1} = 42\,025$ points) and $R = 5$ cm ($N_{T1} = 84\,050$ points). In addition, N_T is calculated in the surrounding healthy tissue comprised in a spherical cap between $R = 2.5$ ($N_{T2} = 17\,651$ points).

Results

In the figure 3. shows the spatial pattern of tissue damage generated by collinear electrode configurations C_{i-Ia} (a), C_{i-Ib} (b), C_{i-Ic} (c) and multiple pairs of electrodes C_{p-I} (d); at distance $d = (0.5, 0.7, 1.0)$ cm.

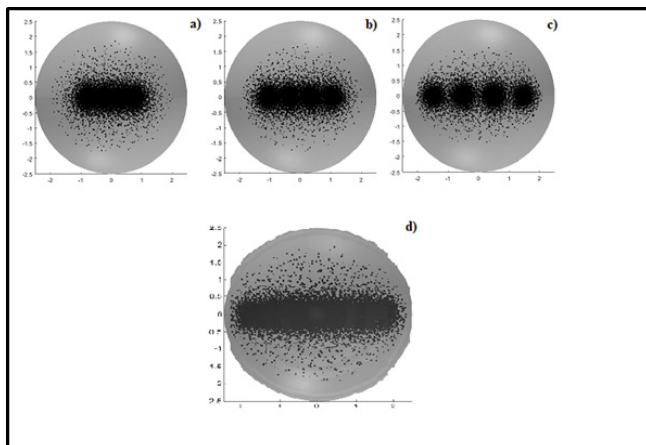


Figure 3 Spatial pattern of tissue damage generated by C_{i-Ia} (a), C_{i-Ib} (b), C_{i-Ic} (c) and multiple pairs of C_{p-I} electrodes inserted perpendicularly in the tumor geometry (d) in the tumor at $R = 2.5$ cm. The parameters of this configuration are presented in Table 1.

Figure 4 shows the spatial pattern of tissue damage generated by single electrode (C_{i-II}) and multiple concentric electrode pairs (C_{p-II}) configurations placed at 45° ; 135° ; 225° and 315° inserted perpendicularly in the tumor geometry (d), with respect to the x-axis, respectively. The parameters of this configuration are presented in Table 1.

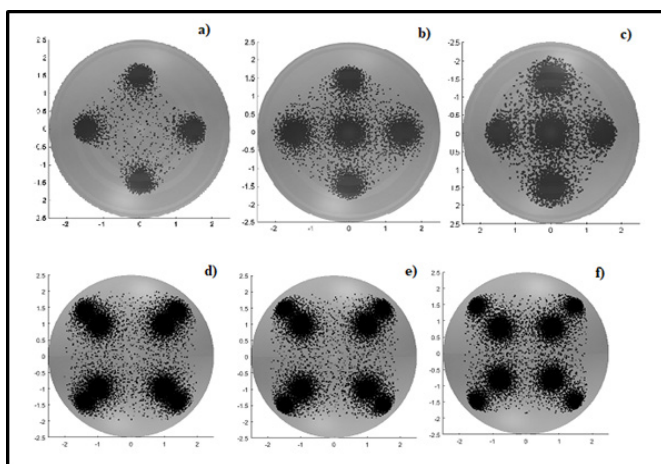


Figure 4 Spatial pattern of tissue damage generated by C_{i-II} and C_{p-II} electrode configurations in tumor radius $R = 2.5$ cm.

Discussion

Figure 3 showed that the highest PDT distribution was generated by the C_{i-Ib} configuration at a distance $d = 0.7$ cm and C_{p-I} , at $d = 1$ cm; for a tumor radius $R = 2.5$ cm. in agreement with the results

of Calzado et al.¹³ Multiple pairs of electrodes behave like multiple single electrodes when $d > 1$ cm, which induce the greatest growth regression and complete remission of F3II mammary carcinoma and survival of male and female BALB/c/Cenp mice.⁸ The other reason is that the anodes (positive electrodes) inserted into the tumor attract the cancer cells, which are negatively charged.^{14,25} Moreover, it is perceived that when R increases the region of induced destruction is smaller. In figure 4 it was demonstrated that the C_{i-II} and C_{p-II} configurations at 45° ; 135° ; 225° and 315° , have around 80% percent of tumor destruction and with the minimum damage to the surrounding healthy tissue; because the temperature (41-45)°C generated by these configurations is induced in the whole volume of the tumor; according to the theory,^{9,14} (results not shown in this study); which corroborates, that it is not only the intensity of the electric current. The (EChT in current mode), the intensity of the electric field (EChT in voltage mode) and the temperature are the essential responsible for tissue damage in tumors, but the toxic products, coming from the electrochemical reactions. Therefore, the most accepted antitumor mechanism of EChT is the electrochemical one, in agreement with what has been documented in the literatura.^{7-11,13,18-23,36,37} Therefore, alterations induced by this therapy in healthy mice are reversible. It promotes a significant delay in the growth of highly invasive and metastatic tumors, since the spatial pattern of tissue damage adopts the same shape as the electrode array and the insertion of multiple concentric straight needle electrodes along the depth and radial direction of tumor growth can enhance the effectiveness of this therapy, as demonstrated experimentally in.³⁸

Conclusion

The lowest PDT values are obtained in the configurations of electrodes inserted individually in the tumor, with a lower percentage C_{i-Ia} ; with respect to C_{p-II} ; for a separation between the electrodes of 0.7 cm. The C_{i-II} and C_{p-II} electrode configurations are the ones that induce the highest tissue damage values and therefore can be used for the treatment of large and deep tumors, which is of vital importance to improve the geometric description of the electrode array and increase the effectiveness in the treatment of tumors.

Acknowledgment

The authors thank the technicians and other colleagues from the National Center for Applied Electromagnetism, the Center for Medical Biophysics and the Faculty of Mechanical Engineering who made this work possible.

Declaration of conflicts of interest

The authors declare that there are no conflicts of interest.

References

1. Delgado IM, Calzado EM, Torres LM. Luis Enrique Bergues Cabrales Distribuciones espaciales del campo eléctrico, temperatura y daño tisular generados por arreglos múltiples de electrodos. 2018.
2. Timmer F, Geboers B, Ruarus AH. Irreversible electroporation for locally advanced pancreatic cancer. *Tech Vasc Interv Radiol*. 2020;23(2):100675.
3. Skandalakis G, Rivera D, Rizea C. Hyperthermia treatment advances for brain tumors. *Int J Hyperthermia*. 2020;37(2):3–19.
4. Densen C. Cancer treatment using laser. *U.S. Patent Application No 11/210,276*, 4. 2021;11(2):906–924.
5. Miripour Z, Aghaee P, Mahdavi R. Nanoporous platinum needle for cancer tumor destruction by EChT and impedance-based intra-therapeutic monitoring. *Nanoscale*. 2020;12(43):22129–22139.

6. O'Brien C, Ignaszak A. Advances in the electrochemical treatment of cancers and tumors: exploring the current trends, advancements, and mechanisms of electrolytic tumor ablation. *Chem Electro Chem*. 2021;7(19):3895–3904.
7. Klein N, Mercadal B, Stehling M. *In vitro* study on the mechanisms of action of electrolytic electroporation (E2). *Bioelectrochemistry*. 2020;133:107482.
8. Xin Y, Zhao H, Zhang W. Electrochemical Therapy of Tumors. *Conference Papers in Science*. 2013; 2013:13.
9. Borges OB, González MM, Rodríguez JLG, et al. Cinética de crecimiento del tumor F3II bajo la acción de diferentes geometrías de múltiples electrodos. Trabajo de tesis de opción al título de Licenciado en Ciencias Farmacéuticas. Universidad de Oriente Facultad de Ciencias Naturales y Exactas Departamento de Farmacia. 2018.
10. Goris NAV, González MM, Borges BO, et al. Efficacy of direct current generated by multiple-electrode arrays on F3II mammary carcinoma: experiment and mathematical modeling. *Journal of Translational Medicine*. 2020;18(1):1–17.
11. Torres LM, Calzado EM, Rodríguez JLG, et al. Distribución espacio-tiempo de frentes de pH generados por un arreglo múltiple de pares electrodos. *Revista Anales de la Academia de Ciencias de Cuba*. 2024;14(2):e1420.
12. Torres LM, Calzado EM, Delgado IMG, Rodríguez JLG, Cabrales LEB. Spatial distributions of electric field, temperature, and pH generated by multiple electrode arrays. *Phys Astron Int J*. 2023;7(2):131–135.
13. Soba A, Suarez C, González MM, et al. Integrated analysis of the potential, electric field, temperature, pH and tissue damage generated by different electrode arrays in a tumor under electrochemical treatment. *Mathematics and Computers in Simulation*. 2018;146:160–176.
14. Calzado EM, Schincab H, Cabrales LEB, et al. Impact of permeabilization and pH effects in the electrochemical treatment of tumors. Experiments and simulations. *Applied Mathematical Modelling*. 2019;74:62–72.
15. Calzado EM, Rodríguez JLG, Cabrales LEB, et al. Simulations of the electrostatic field, temperature, and issue damage generated by multiple electrodes for electrochemical treatment. *Applied, Mathematical Modelling*. 2019;76:699–716.
16. Pupo AEB, Reyes JB, Cabrales LEB, et al. Analytical and numerical. Analytical and numerical a tumor tissue under electrotherapy. *Biomedical Engineering Online*. 2011;10(1):85.
17. Pupo AEB, González MM, Cabrales LEB, et al. 3d current density in tumors and surrounding healthy tissues generated by a system of straight electrode arrays. *Mathematics and Computers in Simulation*. 2017;17:30011–30013.
18. Jiménez RP, Pupo AEB, Cabrales JMB, et al. 3D stationary electric current density into spherical tumor treated with low irect current. *Bioelectromagnetics*. 2011;32(2):120–130.
19. Cabrales LEB, Aguilera AR, Jiménez RP, et al. Mathematical modeling of tumor growth in mice following low-level direct electric current. *Mathematical and Computer in Simulation*. 2008;78:112–120.
20. Li KH, Xin YL, Gu YN, et al. Effects of direct on dog liver: possible mechanisms for tumor electrochemical treatment. *Bioelectromagnetics*. 1997;18(1):2–7.
21. González MM, Aguilar CH, Pacheco FAD, et al. Tissue damage, temperature, and pH induced by different electrode arrays on potato pieces (*Solanum tuberosum* L.). *Front Oncol*. 2018;8:101.
22. Holandino C, Teixeira CAA, Oliveira FAG, et al. Direct electric current treatment modifies mitochondrial function and lipid body content in the A549 cancer cell line. *Bioelectrochemistry*. 2016;111:83–92.
23. Mokhtare A, Reddy MSK, Roodan VA. The role of pH fronts, chlorination and physicochemical reactions in tumor necrosis in the electrochemical treatment of tumors: A numerical study. *Electrochimica Acta*. 2019;307:129–147.
24. Von Euler H, Olsson JM, Hutlenby K, et al. Animal Models for unresectable liver tumor: a histopathologic and ultra-structural study of cellular toxic changes after electrochemical treatment in rat and dog liver. *Bioelectrochemistry*. 2003;59(1–2):89–98.
25. Foster KR, Schwan HP. 1996 Dielectric properties of tissues. In *Handbook of biological effects of electromagnetic fields* (eds. C Polk & E Postow), pp. 68–70. Boca Raton, Florida, CRC Press LLC.
26. Prevez HB, Jimenez AAS, Kindelán JAH, et al. Simulations of surface charge density changes during the untreated solid tumor growth. *R Soc Open Sci*. 2022;9(11):220552.
27. Gilazieva Z, Ponomarev A, Rutland C, et al. Promising applications of tumor spheroids and organoids for personalized medicine. *Cancer*. 2020;12(10):2727.
28. Oria EJR, Cabrales LEB, Reyes JB. Analytical solution of the bioheat equation for thermal response induced by any electrode array in anisotropic tissues with arbitrary shapes containing multiple-tumor nodules. *Revista Mexicana Física*. 2019;65(3):284–290.
29. Castañeda ARS, Del Pozo JM, Ramirez-Torres EE, et al. Spatio temporal dynamics of direct current in treated anisotropic tumors. *Mathematical and Computer in Simulation*. 2023;203:609–632.
30. Shawki MM, Azmy MM, Salama M, et al. Mathematical and deep learning analysis based on tissue dielectric properties at low frequencies predict outcome in human breast cancer. *Technol Health Care*. 2022;30(3):633–645.
31. Yu X, Sun Y, Cai K, et al. Dielectric properties of normal and metastatic lymph nodes ex vivo from lung cancer surgeries. *Bioelectromagnetics*. 2020;41(2):148–155.
32. Sekino M, Ohsaki H, Yamaguchi-Sekino S, et al. Low-frequency conductivity tensor of rat brain tissues inferred from diffusion MRI. *Bioelectromagnetics*. 2009;30(6):489–499.
33. Robinson AJ, Jain A, Sherman HG, et al. Toward hijacking bioelectricity in cancer to develop new bioelectronic medicine. *Advances in Therapy*. 2021;4(3):2000248.
34. Fujita S, Tamazawa M, Kuroda K. Effects of blood perfusion rate on the optimization of RF-capacitive hyperthermia. *IEEE Trans Biomed Eng*. 1998;45(9):1182–1186.
35. Garcia PA, Rossmeisl H, Neal RE, et al. A parametric study delineating irreversible electroporation from thermal damage based on a minimally invasive intracranial procedure. *Biomedical Engineering Online*. 2011;10(1):1–22.
36. Fuhrmann J, Gohlke C, Linke A. Models and numerical methods for electrolyte flows. *Topics in Applied Analysis and Optimisation*. 2019:183–209.
37. Belyy Y, Tereshchenko A, Shatskih A. Clinical procedure for intraocular electrochemical lysis during endoresection. *Ecancermedicalscience*. 2013;7:326.
38. González MM. Daño tisular y cinética tumoral bajo la acción de la electroterapia con diferentes arreglos de electrodos. (Doctoral dissertation, Universidad de Oriente Facultad de Ciencias Naturales y Exactas Departamento de Farmacia). 2017.